'sillimanite'-like structure, respectively) is, however, not practicable. The dark regions within this image are assumed to be due to small domains possessing the average mullite composition. The average size of these domains is about 3·5 nm^2. They are separated by the above-mentioned, linearly arranged (parallel to [102]) white dots. An antiphase relationship between these domains cannot be confirmed for the mullite crystals investigated ($x = 0{\cdot}25$ and $x = 0{\cdot}4$).

The results discussed above show that the intensities of the white dots on the experimental HREM images of the *ac* plane are influenced by all components which modulate the structure of mullite. A proportionality between the intensity of these white dots and of only the concentration of vacancies on certain sites, as assumed by several authors (Nakajima *et al.*, 1975; Ylä-Jääski & Nissen, 1983), cannot be verified.

The assumption of Schryvers *et al.* (1988) that the oxygen vacancies are randomly distributed in mullite crystals obtained by sintering of $3Al_2O_3 + 2ZrSiO_4$ can be best verified by inspecting the b^*c^* and the a^*c^* diffraction pattern. In this case a continuous diffuse background rather than satellite reflexions must be obtained. Moreover, the computer simulations of Schryvers *et al.* (1988) along the *c* axis were unfortunately performed using an average structure model. According to our contrast calculations the intensity differences between the four contrast maxima within the unit cell must vanish owing to an equal vacancy distribution as shown in Fig. 7(*j*). The one-to-one correspondence between the HREM image contrast and the projected crystal structure of mullite, and the correspondence between the vacancy arrangement and the intensity of the simulated contrast features, can, according to the image simulations shown in Fig. 7, best be obtained on the (001) projections.

We thank Professor E. Eberhard for many helpful discussions and Dr H. Schneider (Bonn) for providing the 2:1 mullite single crystals. This work was supported by the Sonderforschungsbereich 173 of the Deutsche Forschungsgemeinschaft.

References

ANGEL, R. J. & PREWITT, C. T. (1986). *Am. Mineral.* **71**, 1476–1482.
ANGEL, R. J. & PREWITT, C. T. (1987). *Acta Cryst.* **B43**, 116–126.
BURNHAM, C. W. (1963). *Carnegie Inst. Washington Yearb.* **62**, 158–165.
BURNHAM, C. W. (1964). *Carnegie Inst. Washington Yearb.* **63**, 223–227.
CAMERON, W. E. (1977). *Am. Mineral.* **62**, 747–755.
COWLEY, J. M. (1975). *Diffraction Physics.* Amsterdam: North-Holland.
COWLEY, J. M. & MOODIE, A. F. (1957). *Acta Cryst.* **10**, 609–619.
DUROVIC, S. (1969). *Chem. Zvesti*, **23**, 113–128.
DUROVIC, S. & FEJDI, P. (1976). *Silikaty*, **20**, 97–112.
EBERHARD, E., HAMID RAHMAN, S. & WEICHERT, H.-T. (1986). *Z. Kristallogr.* **174**, 44–46.
GJØNNES, J. & MOODIE, A. F. (1965). *Acta Cryst.* **19**, 65–67.
GOODMAN, P. & MOODIE, A. F. (1974). *Acta Cryst.* A**30**, 280–290.
HAMID RAHMAN, S. (1988*a*). *Z. Kristallogr.* **186**, 113–116.
HAMID RAHMAN, S. (1988*b*). *Z. Kristallogr.* **186**, 116–119.
HEINE, V. & MCCONNELL, J. D. C. (1984). *J. Phys. C*, **17**, 1199–1220.
KUMAO, A., NISSEN, H.-U. & WESSICKEN, R. (1987). *Acta Cryst.* B**43**, 326–333.
MCCONNELL, J. D. C. & HEINE, V. (1984). *Acta Cryst.* A**40**, 473–482.
MCCONNELL, J. D. C. & HEINE, V. (1985). *Phys. Rev. B*, **31**, 6140–6142.
NAKAJIMA, Y., MORIMOTO, N. & WATANABE, E. (1975). *Proc. Jpn Acad.* **51**, 173–178.
SAALFELD, H. (1962). *Transactions of the* VIII *International Ceramic Congress, Copenhagen*, pp. 71–74.
SAALFELD, H. & GUSE, W. (1981). *Neues Jahrb. Mineral. Monatsh.* **4**, 145–150.
SCHRYVERS, D., SRIKRISHNA, K., O'KEEFE, M. A. & THOMAS, G. (1988). *J. Mater. Res.* 3(6), 1355–1361.
SELF, P. G., CLAISHER, R. W. & SPARGO, A. E. C. (1985). *Ultramicroscopy*, **18**, 49–62.
SMITH, D. J., BURSIL, L. A. & WOOD, G. J. (1985). *Ultramicroscopy*, **16**, 19–32.
TANAKA, N. & COWLEY, J. M. (1987). *Acta Cryst.* A**43**, 337–346.
TAYLOR, W. H. (1928). *Z. Kristallogr.* **68**, 503–521.
YLÄ-JÄÄSKI, J. & NISSEN, H.-U. (1983). *Phys. Chem. Miner.* **10**, 47–54.

Acta Cryst. (1990). B**46**, 149–153

A Generalized Description of Ideal Crystal Structures for Monatomic Solids

BY W. L. NG

Department of Chemistry, University of Malaya, 59100 *Kuala Lumpur, Malaysia*

(*Received* 3 *July* 1989; *accepted* 27 *October* 1989)

Abstract

A variety of ideal close-packing structures were constructed using a stacking mechanism with rhombus, square and triangular nets of atoms interrelated by a common angular parameter. The structural features of the resulting space lattice are greatly influenced by the sequence and mode of stacking and the type of

0108-7681/90/020149-05$03.00

net. It was found that stacking by *AB* sequence yields structures of highest symmetry whereas stacking *via* a central mode results in structures of higher coordination number and packing density. The importance of symmetry in determining the most probable structures is highlighted and a generalized description of ideal close-packing structures is proposed.

1. Introduction

The concept of closest packing of rigid atoms was used (Barlow, 1883) in the study of crystal structure. It was later developed into eutectic packing of atoms (O'Keeffe, 1977) to permit larger atoms to occupy interstitial sites, and such structures are widely adopted by intermetallic and ionic compounds (Gehman, 1963). Monatomic elements are expected to crystallize in h.c.p. and c.c.p. structures. The description of h.c.p. as a stack of hexagonal closest packing layers can be easily understood. It is, however, not intuitively obvious how hexagonal layers can be stacked into a cubic structure. On the other hand, the adoption of b.c.c. structure by some 27 elements is regarded as an anomaly (Ho & Douglas, 1968) as it does not contain a closest packing layer. Of late, h.c.p., c.c.p. and b.c.c. structures have been described (Figueiredo & Lima-de-Faria, 1978) as stacks of hexagonal, square and rhombus layers, respectively. It was shown (Lima-de-Faria, 1978) that the structures depend on (i) the ways in which atoms are arranged in the layer and (ii) the manner in which identical layers are stacked together. Recently, primitive tetragonal packing (p.t.p.) and body-centered tetragonal (b.c.t.) structures have been found in some oxides (West, 1987). This paper presents a unified description of all close-packing structures. The effects of the stacking of identical layers on the symmetry, packing density and coordination number of the resulting space lattice are critically discussed.

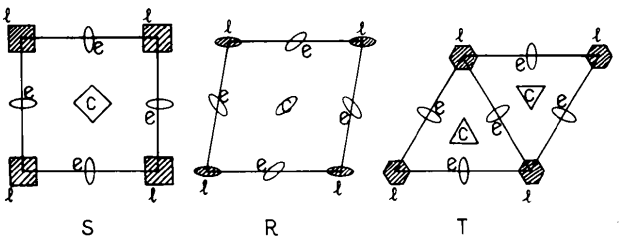

Fig. 1. Unit cells of the three planar lattices showing their symmetry axes at the lattice sites (shaded) and valley sites (unshaded): diad, ⬭; triad, △; tetrad, □; hexad, ⬡; *c*, central-valley site; *e*, edge-valley site; *l*, lattice site.

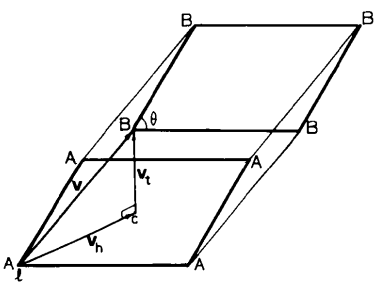

Fig. 2. Two rhombus nets (*A*, *B*) stacked *via* the central mode. The vertical component $\mathbf{V}_t$ of the stacking vector $\mathbf{V}$ forms the height of a triclinic unit cell of edge $2r$.

2. Stacking mechanism

There are five types of planar nets (Buerger, 1971) of which only three are applicable to a closely packed monatomic layer. These are rhombus, square and triangular nets (Fig. 1). Two types of periodic depression exist on both sides of the layer. They are a central valley at the center and edge valleys at the mid-edges of the unit cell or sub-cell of the net. Nets are stacked on top of one another by a stacking vector $\mathbf{V}$ at the lattice site (Fig. 2). This vector has two componenets: (i) horizontal $\mathbf{V}_h$ which indicates lateral displacement of the nets and (ii) vertical $\mathbf{V}_t$ which measures interlayer separation. Equation (1) relates the two components to the radius r of the atom:

$$\mathbf{V}_h^2 + \mathbf{V}_t^2 = 4r^2. \qquad (1)$$

Stacking of layers involves the fitting of atoms of one layer into the valleys of its two sandwiching layers to maximize the use of space in accordance with Laves principle (Laves, 1955). There are two modes of stacking involving either central- or edge-valley sites. Only one set of valleys can be occupied at a time by atoms of adjacent layers. In either a square or a rhombus net the multiplicity of the central valley is 1. Thus the orientations of the two sandwiching layers have to be the same (*A*, *A*) but different from that of the layer (*B*) being sandwiched. This stacking sequence is denoted by *AB*.

For a central valley in a triangular net (or an edge valley in either a square or a rhombus net) the multiplicity is 2. The orientation of the two sandwiching layers can either be the same (*A*, *A*) or different (*A*, *C*) with respect to the layer (*B*) being sandwiched. The two sequences are thus denoted by *AB* and *ABC*, respectively. By analogy, the three sequences of stacking a triangular net *via* the edge mode (multiplicity = 3) are *AB*, *ABC* and *ABCD*. In general, there are m sequences for a valley of m multiplicities. It is interesting to note that although the nets are precursors, they are, however, not preformers of the resulting space lattices. It is a com-

bination of the mode and sequence of stacking and the type of net that determines the structure of the lattice. Thus a structural symbol such as X_q^i is self-explanatory and fully representative of the ways by which a structure is generated. In this symbol, X denotes the type of planar nets (R for rhombus, S for square, T for triangular), i denotes the mode of stacking (c for central mode, e for edge mode), and q denotes the sequence of stacking (AB, ABC or $ABCD$).

3. Ideal crystal structures

3.1. *Stacking via the central mode*

(*a*) *Square net.* The tetrad symmetry at both the lattice and valley sites survives in the stacking by AB sequence. All central-valley sites are converted into regular octahedral holes. Each layer is a mirror plane since it is stacked above and below by layers of identical spatial configuration. In addition, there are four triads emanating from the hole. The resulting lattice thus belongs to the space group $Fm3m$ and is a face-centered cubic closest packing (c.c.p.) structure.

(*b*) *Rhombus net.* Both the lattice and valley sites have diad symmetry. Three orthogonal mirror planes and a tetrad along the short diagonal of the rhombus net are created. The resulting lattice has space-group symmetry $I4/mmm$ and is a body-centered tetragonal (b.c.t.) structure.

(*c*) *Triangular net.* The symmetry axes at the lattice and valley sites are hexad and triad, respectively. In AB sequence, the octahedral holes at the unoccupied valley sites form empty channels normal to the nets. Because adjoining nets are staggered with respect to each other, the improper triads ($\bar{3}$) at the unoccupied valley sites of the net are converted into screw hexads 6_3. The resulting primitive lattice belongs to the space group $P6_3/mmm$ and is a hexagonal closest packing (h.c.p.) structure. In ABC sequence, there are four triads at the center of the octahedral hole. The resulting lattice has space symmetry $Fm3m$ and is a cubic closest packing (c.c.p.) structure.

3.2. *Stacking via the edge mode*

(*a*) *Square net.* The lattice and valley sites have tetrad and diad symmetry, respectively. In AB sequence, a set of vertical triangular nets is created. This gives rise to a set of diads at their lines of intersection and a set of hexads normal to the vertical triangular nets. The resulting lattice belongs to space group $P6/mmm$ and is a simple hexagonal packing (s.h.p.) structure. In ABC sequence, the tetrads at the lattice sites disappear leaving diads as the principal symmetry axes. The lattice also possesses two orthogonal mirror planes which contain the axes. The resulting lattice thus belongs to space group $P2mm$ and is a primitive orthorhombic close-packing (o.c.p.) structure.

(*b*) *Rhombus net.* Diads exist at both the lattice and valley sites. In AB sequence, a set of vertical triangular nets is created. The nets are displaced laterally so that the hexads associated with each net are completely removed. The resulting lattice has vertical diads at its lattice sites and mirror planes on the stacking layers. It has the centrosymmetrical space group $C2/m$ and is a monoclinic close-packing (m.c.p.) structure. In ABC sequence, the resulting lattice consists, however, of three interlacing primitive monoclinic sub-lattices and has the centrosymmetrical space group $P2/m$. It is a monoclinic close-packing (m.c.p.) structure.

(*c*) *Triangular net.* In AB sequence, the hexads at the lattice sites are converted into diads while the diads at the valley sites remain unchanged. A set of vertical triangular nets is created. At each line of intersection a tetrad is formed. This tetrad is the principal axis of the lattice which also has three orthogonal mirror planes. The space group is thus $I4/mmm$ and the lattice is a body-centered tetragonal (b.c.t.) structure. In either ABC or $ABCD$ sequence, the axial symmetry of the resulting lattice is reduced to a set of diads. It consists of two and three sub-lattices, respectively. In either case, a simple monoclinic packing (s.m.p.) structure of space group $P2$ is created.

4. Structural features

4.1. *Symmetry, packing density and coordination number*

The symmetry of the net is readily modified when identical nets are stacked together. Its modification depends on both the sequence and mode of stacking. For example, in AB sequence each layer becomes a mirror plane. When intersected by a vertical axis, the plane generates inversion centers at the points of intersection. The translational symmetry of the lattice converts a proper axis into an improper axis or a screw axis (*e.g.* 6_3 and $\bar{3}$ present in T_{AB}^c). On the other hand, the layer does not become a mirror plane in either the ABC or $ABCD$ sequence of stacking. A new axis may be added (*e.g.* triads created in S_{AB}^c) or an existing one may be removed (*e.g.* hexads absent from T_{AB}^e) such that the resulting space lattice bears little or no resemblance at all in symmetry to the nets from which it was built (see Table 1).

The percentage packing density $\%P(\theta)$ of a given structure can be obtained by reference to a two-layer stacking (Fig. 2) using the generalized equation (2):

$$\%P(\theta) = (100\pi/3)a(1+\cos\theta)^{-b}/\sin\theta\ \% \qquad (2)$$

Table 1. *Structural parameters of ideal crystal structures*

Structure symbol	Type of structure*	Space group	% packing density	Coordination number	Angular parameter (°)
S^c_{AB}	c.c.p.	$Fm3m$	74·0	12	90
T^c_{ABC}	c.c.p.	$Fm3m$	74·0	12	60
T^h_{AB}	h.c.p.	$P6_3/mm$	74·0	12	60
T^t_{AB}	b.c.t.	$I4/mmm$	69·8	10	60
R^t_{AB}	b.c.t.	$I4/mmm$	$68·0 < P(\theta) < 74·0$	8	$90 < \theta < 60$
R'^c_{AB}	b.c.c.	$Im3m$	68·0	8	70°32′
S^h_{AB}	s.h.p.	$P6/mmm$	60·5	8	90
R^m_{AB}	m.c.p.	$C2/m$	$60·5 < P(\theta) < 69·8$	8	$90 < \theta < 60$
S^o_{ABC}	o.c.p.	$P2mm$	60·5	8	90
R^m_{ABC}	m.c.p.	$P2/m$	$60·5 < P(\theta) < 69·8$	8	$90 < \theta < 60$
T^s_{ABC}, T^s_{ABCD}	s.m.p.	$P2$	69·8	10	60

* c.c.p. cubic closest packing, h.c.p. hexagonal closest packing, b.c.t. body-centered tetragonal packing, b.c.c. body-centered cubic packing, s.h.p. simple hexagonal packing, m.c.p. monoclinic closest packing, o.c.p. orthorhombic closest packing, s.m.p. simple monoclinic packing.

Table 2. *Characterstic constants a and b of equation (2) for the percentage packing density*

Stacking mode	a	b	Planar net
Central	0·707	0·500	Rhombus
	0·707	0·500	Square
	0·612	0	Triangular
Edge	0·577	0	All

where a and b are constants characteristic of the mode of stacking and type of nets (Table 2). Geometrically both the square and triangular nets can be considered to be derived from a rhombus net (Fig. 3) with its oblique angle θ equal to 90 and 60°, respectively. In transforming a rhombus into a triangular net, its central valleys are converted into a set of edge valleys with the simultaneous creation of two sets of central-valley sites. The dependence of packing density on the angular parameter and the mode of stacking is obvious from Fig. 4, which shows unequivocally that stacking *via* the central mode yields structures of higher packing density throughout the entire range of θ.

The coordination number L of the space lattice can be obtained by reference to that of the atom (N) and valley (n) in the net from which the lattice is generated using equation (3):

$$L = N + 2n. \qquad (3)$$

The factor 2 takes care of the two sandwiching layers. In stacking *via* the central mode, n is 2, 3 and 4 for rhombus, triangular and square nets, respectively. In stacking *via* the edge mode, n is 2 for all nets.

4.2. *Effect of sequence and mode of stacking*

$\%P(\theta)$ and L are independent of the sequence of stacking [equations (2) and (3)]. In stacking involving a valley of multiplicity m, there are m sequences which give rise to m close-packing structures of the

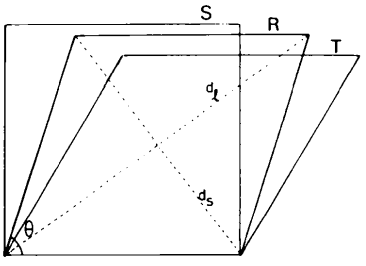

Fig. 3. The correlation of square, rhombus and triangular nets *via* the angular parameter θ. Square net, $\theta = 90°$; triangular net, $\theta = 60°$; rhombus net, $90 > \theta > 60°$.

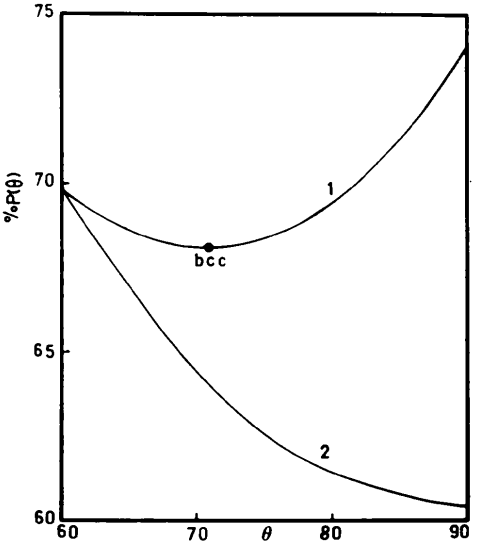

Fig. 4. Plot of percentage packing density $\%P(\theta)$ *versus* the angular parameter θ (°) for all ideal space lattices derived from stacking planar nets *via* the central mode (curve 1) and the edge mode (curve 2).

same $\%P(\theta)$ and L but different structure and symmetry. Among the m sequences, stacking by AB sequence yields structures of the highest symmetry. Between the two modes of stacking, stacking *via* the central mode results in structures of consistently higher $\%P(\theta)$ (Fig. 4) and L (Table 1). Hence, based on Laves principle (Laves, 1955) of maximum packing density, highest symmetry and largest coordination number, the three most probable structures arising from the three basic nets should be R^c_{AB}, S^c_{AB} and T^c_{AB}, which are b.c.t., c.c.p. and h.c.p., respectively. This principle is fully exemplified by the last two structures which are also the closest packing structures.

5. The b.c.c. structure

The packing density of a b.c.t. structure has its minimum value of 68% at $\theta = 70° 32'$ (curve 1 in Fig. 4). The equation below relates θ to its axial ratio c/a:

$$c/a = 0{\cdot}71(1 + \cos\theta)/\sin\theta. \quad (4)$$

At 70° 32′ the ratio equals 1 and b.c.t. becomes b.c.c. It is interesting to note that although b.c.t. is more densely packed than b.c.c., it rarely occurs whereas the latter is the third most frequently adopted structure after c.c.p. and h.c.p. This preferential adoption of b.c.c. is obviously due to its higher symmetry (isometric). Thus symmetry factors strongly outweigh packing density in determining the most probable structure. This rationale is consistent with the central force of interaction which favours highly symmetrical arrangements rather then the densest packing structures. For example, simple hexagonal (s.h.p.) structure is occasionally adopted (Pearson, 1972) even though its $\%P(\theta)$ is smaller *vis-à-vis* other close-packing structures of lower symmetry.

References

BARLOW, W. (1883). *Nature (London)*, **29**, 186–188, 205–207.

BUERGER, M. J. (1971). *Introduction to Crystal Geometry*, p. 36. New York: McGraw-Hill.

FIGUEIREDO, M. O. & LIMA-DE-FARIA, J. (1978). *Z. Kristallogr.* **148**, 7–19.

GEHMAN, W. G. (1963). *J. Chem. Educ.* **40**, 54–60.

HO, S. M. & DOUGLAS, B. E. (1968). *J. Chem. Educ.* **45**, 474–476.

LAVES, F. (1955). *Theory of Alloy Phases*, p. 124. Cleveland: American Society for Metals.

LIMA-DE-FARIA, J. (1978). *Z. Kristallogr.* **148**, 1–5.

O'KEEFFE, M. (1977). *Acta Cryst.* A**33**, 924–927.

PEARSON, W. B. (1972). *The Crystal Chemistry and Physics of Metals and Alloys*, p. 303. New York: Wiley–Interscience.

WEST A. R. (1987). *Solid State Chemistry and its Applications*, p. 225. New York: John Wiley.

Acta Cryst. (1990). B**46**, 153–159

Modulated Structure of $(Ta_{0.72}Nb_{0.28})Te_4$

BY D. KUCHARCZYK

Institute for Low Temperature and Structure Research, Polish Academy of Sciences, pl. Katedralny 1, 50–950 *Wrocław, Poland*

A. BUDKOWSKI

Institute of Physics, Jagellonian University, Reymonta 4, 30–059 *Kraków, Poland*

F. W. BOSWELL

Guelph-Waterloo Program for Graduate Work in Physics, University of Waterloo, Ontario, Canada N2L 3G1

AND A. PRODAN AND V. MARINKOVIĆ

'J. Stefan' Institute, Jamova 39, *and Department of Metallurgy, University of Ljubljana*, 61000 *Ljubljana, Slovenia, Yugoslavia*

(*Received* 16 *June* 1989; *accepted* 23 *October* 1989)

Abstract

The commensurately modulated structure of tantalum niobium tetratelluride, $(Ta_{0.72}Nb_{0.28})Te_4$, was determined by X-ray (Mo $K\alpha$, $\lambda = 0{\cdot}71069$ Å) diffraction at room temperature. The symmetry is described by superspace group $P\,^{P4/ncc}_{1\ 111}(00\gamma)$ $(t = 0)$ with a $(2a \times 2a \times c)$ basic unit cell or equivalently by

0108-7681/90/020153-07$03.00